UCRL-CONF-215123

LAWRENCE
LIVERMORE
NATIONAL
LABORATORY

Scaling of Pressure with Intensity in Laser-Driven Shocks and Effects of Hot X-ray Preheat

J. D. Colvin, D. H. Kalantar

September 7, 2005

American Physical Society Topical Conference on Shock Compression of Condensed Matter
Baltimore, MD, United States
July 31, 2005 through August 5, 2005

SCALING OF PRESSURE WITH INTENSITY IN LASER-DRIVEN SHOCKS AND EFFECTS OF HOT X-RAY PREHEAT

Jeffrey D. Colvin and Daniel H. Kalantar

Lawrence Livermore National Laboratory, L-356, P.O. Box 808, Livermore, CA 94551

Abstract. To drive shocks into solids with a laser we either illuminate the material directly, or to get higher pressures, illuminate a plastic ablator that overlays the material of interest. In both cases the illumination intensity is low, $\ll 10^{13}$ W/cm^2, compared to that for traditional laser fusion targets. In this regime, the laser beam creates and interacts with a collisional, rather than a collisionless, plasma. We present scaling relationships for shock pressure with intensity derived from simulations for this low-intensity collisional plasma regime. In addition, sometimes the plastic-ablator targets have a thin flash-coating of Al on the plastic surface as a shine-through barrier; this Al layer can be a source of hot x-ray preheat. We discuss how the preheat affects the shock pressure, with application to simulating VISAR measurements from experiments conducted on various lasers on shock compression of Fe.

Keywords: iron, high-pressure solid-state phase transformations, x-ray preheat, shock waves in solids, laser-target interactions.
PACS: 52.38Dx, 52.50Jm, 61.10Nz, 61.50Ks, 62.50+p, 64.70Kb.

SCALING OF PRESSURE WITH INTENSITY

For laser-driven shocks the absorption physics and shock pressure depend on the laser intensity and wavelength. For intensities below about 10^{10} W/cm^2, the very low intensity regime, the laser beam interacts with solid, liquid, and vaporized material, or a very cool plasma. In this intensity regime the technique of tamped ablation [1] is used; i.e., the laser light first passes through a transparent dielectric tamper overlaying the sample to be driven. In this case the pressure in the sample scales as the square root of the laser intensity.

For intensities above about 10^{13} W/cm^2, the high intensity regime, the laser beam creates and interacts with a collisionless coronal plasma. This is the regime of inertial confinement fusion [2]. In this regime of intensities, the shock pressure scales as the two-thirds power of the laser intensity.

Both the tamped ablation regime at very low intensities and the ICF regime at high intensities have been very well studied experimentally and computationally. It is the intermediate intensity regime, intensities between about 10^{10} W/cm^2 and about 10^{13} W/cm^2, a regime of intensities in which the laser beam is interacting with a collisional plasma, that has not been well studied, and which is the subject of the work reported here.

The laser beam heats a collisional ablated plasma differently than a collisionless one. At high intensities ($>10^{13}$ W/cm^2) a coronal plasma with density below the critical density is formed, and the laser beam heats this collisionless plasma to near isothermal conditions. In this collisionless plasma, where the electron-ion collision rate is less than the plasma frequency, the temperature can be approximated by using an electron flux limit in solving the transport equation. It can be shown from this approximation that the pressure scales as the two-thirds power of the intensity [2]. This scaling has been verified with simulation [2].

This approximation is no longer valid in a collisional plasma, so the scaling of pressure with intensity may be different. We have determined the scaling with simulations using the radiation-hydrodynamics code Lasnex [3].

We have modeled experiments in which iron was directly driven with and without a parylene-N (C_8H_8) or parylene-C (C_8H_7Cl) ablator. The experiments were conducted on the Vulcan laser at Oxford University with a 1-μm beam, on the Janus laser at LLNL with a ½-μm beam, and on the Omega laser at the University of Rochester with a 1/3-μm beam. Details of the experiments are presented in another paper in these Proceedings [4]. We specifically modeled the ablator+Fe targets in order to determine the scaling of pressure in the Fe with beam intensity and laser wavelength.

A power-law fit to the Lasnex simulations gives a near-linear scaling of pressure with beam intensity; specifically, we find

$$P^*=41.5\{I(\mathrm{W/cm^2})/3.16\mathrm{x}10^{10}\}^{0.9}\{\lambda_0/\lambda\}^{\alpha(\lambda)}\ \mathrm{kbar}$$

Here P* is the pressure at the front face of the Fe, I is the beam intensity, λ the laser wavelength, and λ_0=1/3 μm. The scaling exponent for wavelength is itself wavelength dependent.

HOT X-RAY PREHEAT

Since parylene is transparent to the laser light at very low intensities (i.e., at early times when the pulse is rising to its peak intensity) a thin (0.1 μm) overcoat of Al was added to the ablator to prevent shine-through and direct preheating of the Fe by the laser beam. While the addition of the Al overcoat to the plastic ablator mitigates one preheat problem, it creates another. The laser-heated Al adds an indirect source of x-ray preheat. That is, the laser-heating of the Al overcoat generates a significant non-thermal flux of soft (~200 eV) x-rays. Some fraction of this flux transmits through the parylene ablator and is absorbed at the front surface of the iron, heating it and raising its pressure before the arrival of the ablatively driven shock.

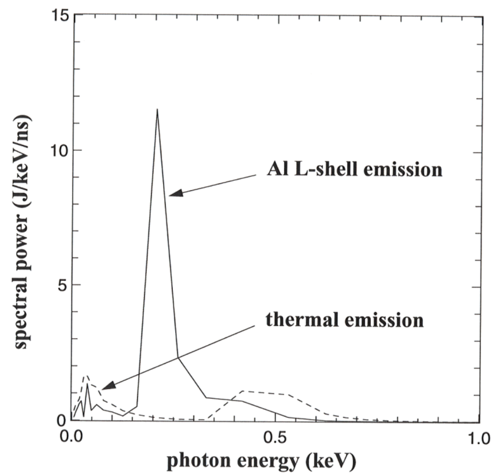

Figure 1. Simulated spectral power crossing the front face of the parylene-N for an intensity of $2\mathrm{x}10^{11}$ W/cm^2 incident on a target of 15 μm parylene-N on 250 μm Fe, with (solid curve) and without (dashed curve) a 0.1-μm Al overcoat on the ablator.

In Fig. 1 we show the spectral power crossing the front face of the parylene-N as a function of photon energy, determined in simulations of one of the Omega experiments in which 117 J of 1/3–μm laser light in a 6-ns-square pulse (I = $2\mathrm{x}10^{11}$ W/cm^2) was incident on a target of 15 μm parylene-N on 250 μm iron, both with (the solid curve) and without (the dashed curve) the 0.1-μm Al shine through barrier.

As is evident in Fig. 1, more absorption in the bare parylene means the target without the Al overcoat heats up hotter and produces more thermal emission, but the target with the Al overcoat produces a large flux of Al L-shell emission at higher photon energy.

The different spectra lead to different heating of both the plastic ablator and the iron. In Fig. 2 we show the simulated temperature profiles in the target at 6 ns, the end of the laser pulse, for the same target and drive configuration as in Fig.. 1, and for different opacities (κ) in the parylene ablator.

The laser energy is entirely absorbed in only the outer ~1 μm of the ablator. This outer layer of the ablator heats up to ~80 eV in the bare target

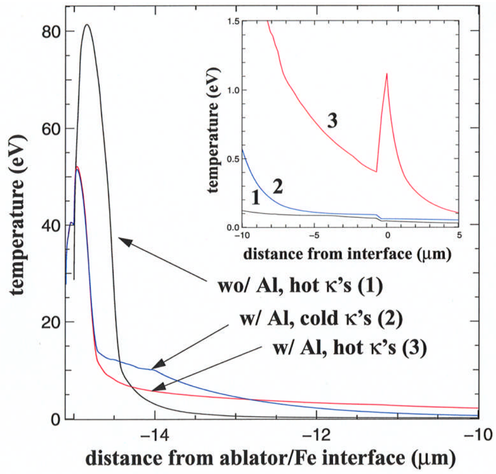

Figure 2. Simulated temperature (eV) vs original Lagrangian distance from ablator/Fe interface (µm) at 6 ns for the target and drive of Fig. 1. Simulations with and without the Al, and for different parylene opacities (κ).

(without the Al), and to ~52 eV in the target with the Al overcoat (the Al itself heats to only ~40 eV). In the bare target the ablator/Fe interface stays cold (i.e., the thermal flux from the outer ~1 µm of the ablator is entirely absorbed in the ablator). In contrast, some of the non-thermal flux from this hot outer layer in the target with the Al overcoat does get through to the ablator/Fe interface, heating it. The radiative preheating of the Fe is strongly dependent on the ablator opacity. Using hot ablator opacities everywhere, the front face of the iron heats to over 1 eV; using cold opacities it heats to just under 0.1 eV.

The hot opacities better describe the thermal flux transport in the hot outer ~1 µm of the ablator. For the hot parylene opacity we use XSN, a statistical screened hydrogenic average atom model. XSN is reasonably accurate at higher temperatures (>10 eV) where free-free transitions dominate the opacity, the outer ~1 µm. XSN is not accurate at lower temperatures where bound-bound and bound-free transitions are important. For the cold parylene opacity we use tabulated cold (zero-temperature) opacities. This is a good approximation for the non-thermal flux since the opacity of 200 eV photons at these low temperatures is better described by cold than by XSN opacities.

Additionally, we use a low-temperature thermal conductivity model in the parylene ablator.

In order to get a handle on the correct ablator opacities to use in the simulations, we compare the simulations to both the *in situ* diffraction data and the VISAR data. Kalantar *et al.* have discussed the diffraction data [4, 5], in which 6.7 keV x-rays generated by the interaction of a separate laser beam with an Fe back light foil diffracted from a thin surface layer of the Fe at and near the ablator/Fe interface, and were recorded on a large-area film detector. These measurements show that the Fe transformed, under shock compression, to the ε (hcp) phase, not to the higher-temperature γ (fcc) phase.

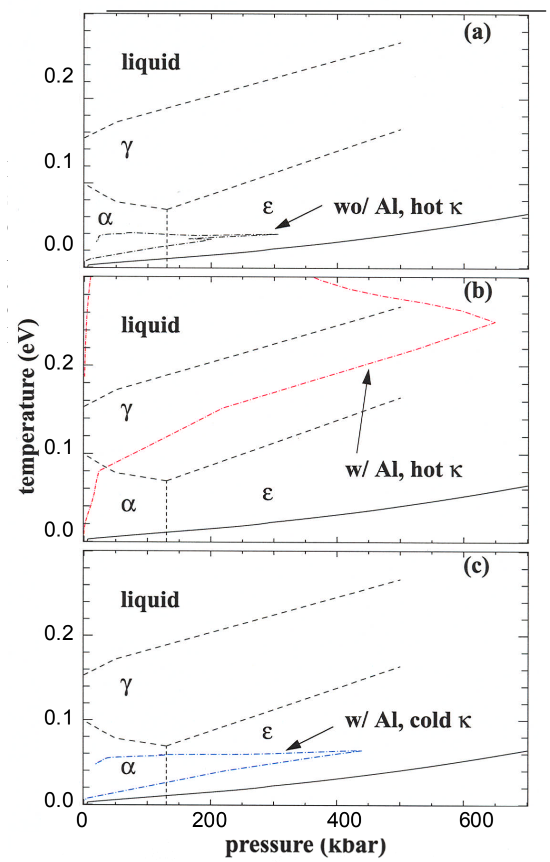

Figure 3. Simulated trajectory in temperature-pressure space of the front 3 µm of the Fe, overlaid on the equilibrium phase diagram for targets a) without Al and with hot ablator opacities; b) with Al and hot ablator opacities; and c) with Al and cold ablator opacities. The solid curve is the zero-temperature Hugoniot.

As seen in Fig. 3, there is clearly too much Al x-ray preheat of the Fe using the hot ablator opacities. In this simulation the trajectory of the front 3 μm of the Fe never crosses the equilibrium α-to-ε phase boundary. With this much preheat, the Fe would heat up enough to first cross the α-to-γ equilibrium phase boundary. Since this is inconsistent with the diffraction data, the use of the hot parylene opacities cannot be right, as expected. The other two cases shown in Fig. 3 (no Al and hence no preheat, and Al with cold ablator opacities) are both consistent with the diffraction data, but there is a ~50% difference in the peak pressures for these two cases.

In order to distinguish between these two cases (no Al and hence no preheat, and Al with cold ablator opacities) we next compare the simulations to the VISAR data. The VISAR diagnostic is a velocity interferometer which records the material velocity as a function of time at the free surface of the Fe [6]. In comparing the simulations with VISAR data, shown in Fig. 4, we see that the simulations with the cold parylene opacities everywhere are consistent with the VISAR data. A simulation without non-thermal flux from an Al overcoat gives a peak free-surface velocity that is too low compared to the data, and a simulation with the Al and hot ablator opacities gives a peak free-surface velocity that is too high. For the simulation with the Al and cold ablator opacities, there is a good match in amplitude but not in timing of the plastic wave.

There is an even better match to the VISAR data when we account for the plasticity kinetics and material spall, also shown in Fig. 4. The simulation with plasticity kinetics and spall models includes a model for plasticity kinetics of Gilman [7], and an unpublished model of spall of Minich, based on percolation theory. Details of the plasticity kinetics and spall modeling will be published separately. We conclude that properly accounting for preheat, as well as properly accounting for the kinetics of the plasticity transition, are necessary in modeling laser-driven shocks in solids.

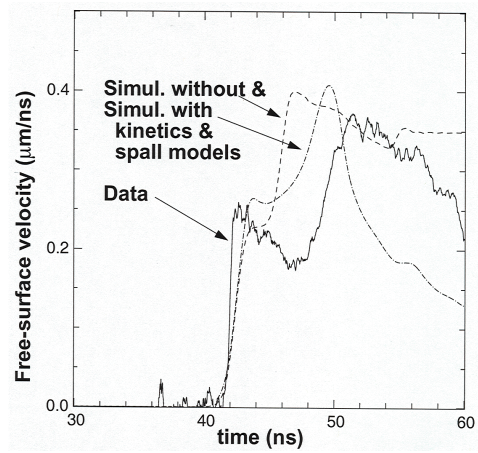

Figure 4. Simulated velocity history of the free surface of Fe compared to data. Simulations were done with Al and cold ablator opacities, both with and without plasticity kinetics and spall models in the simulation.

ACKNOWLEDGEMENTS

This work was performed under the auspices of the U.S. Dept. of Energy by UC Lawrence Livermore National Laboratory under Contract No. W-7405-Eng-48. The authors are indebted to Dr. Roger Minich of LLNL for doing the simulation with the plasticity kinetics and spall models, and for numerous enlightening discussions on the behavior of shock-compressed solids.

REFERENCES

1. Colvin, J. D., Ault, E. R., King, W. E., and Zimmerman, I. H., Phys. Plasmas **10**, 2940, 2003.
2. Lindl, J., Phys. Plasmas **2**, 3933, 1995.
3. Zimmerman, G. B. and Kruer, W. L., Comments Plasma Phys. Control. Fusion **2**, 51, 1975.
4. Kalantar, D. H. et al., paper K6.01 in these Proceedings.
5. Kalantar, D. H. et al., Phys. Rev. Lett. **95**, 075502 (2005).
6. Barker, L. M., and Hollenback, R. E., J. Appl. Phys. **43**, 4669, 1972.
7. Gilman, J. J., J. Appl. Phys. **36**, 2772, 1965.